

## A NEW METHOD FOR ONLINE MONITORING AND TRIMMING OF PYROMETER MEASUREMENTS IN HIGH PERFORMANCE TURBO ENGINES

**Hassan Abdullahi<sup>★</sup>, Michael Kotulla<sup>\*</sup>, Stephan Staudacher<sup>\*</sup>**

<sup>★</sup> MTU Aero Engines GmbH, Dachauer Str. 665, 80995 München, Germany

<sup>\*</sup> University of Stuttgart, Pfaffenwaldring 6, 70569 Stuttgart, Germany

### Abstract

The measurement of gas temperatures in modern engines is indispensable for control and monitoring purposes. In hot areas like the high-pressure turbine pyrometers are well suited for this measurement. They are used for measuring of blade surface temperatures. With the application of pyrometers there are however considerable problems concerning the accuracy and repeatability of the measurements with the consequence that the engine thrust potential cannot be completely utilized, as an adequately large safety margin has to be considered.

In this research work, a new method will be presented that has been developed for a two-spool engine with afterburner. As input the method uses parameters, which are already being measured with the standard instrumentation of the engine. With this method an in-flight online check of the pyrometer measurements is possible. The analysis results of extensive data gained from engine testing at different ambient and flight conditions on the bench test-bed and altitude test facility test-bed as well as in flight show that significant improvement of the measurement accuracy and repeatability can be achieved.

### Nomenclature

<i>a</i>	trim parameter
<i>A</i>	flow area
<i>b</i>	trim parameter
<i>h</i>	enthalpy
<i>N</i>	rotational speed
<i>P</i>	pressure

<i>SOT</i>	temperature at HPT stator exit
<i>t</i>	flight time
<i>T</i>	temperature
<i>W</i>	mass flow
<i>Y</i>	parameter
$\alpha$	fuel heat value
$\gamma$	gamma, gas property
$\varepsilon$	iteration break limit
$\eta$	combustion efficiency
$\sigma$	standard deviation
$\epsilon$	element

### Subscripts

<i>3</i>	compressor exit station
<i>405</i>	HPT nozzle throat station
<i>41</i>	HPT stator exit station
<i>BL</i>	bleed air
<i>C</i>	corrected to standard day conditions
<i>CL</i>	cooling air
<i>D</i>	DECU value
<i>F</i>	fuel
<i>L</i>	low-pressure spool
<i>P</i>	pyrometer
<i>ref</i>	reference value
<i>R</i>	gas constant
<i>T</i>	available on test-bed only
<i>u</i>	lower fuel heat value

### Abbreviations

ATF	altitude test facility
DECU	digital engine control unit
HPT	high-pressure turbine
ISA-SLS	standard atmosphere and sea level static

## 1. Introduction

The need for engines with small dimensions and higher efficiency leads to the development of engines operating at their thermal stress limits, thus the measurement of the gas temperatures is very important. In modern engines the gas temperatures of the high-pressure turbines HPT are so high that at present they can only be measured using pyrometers.

A pyrometer measures the heat radiation of the turbine blade surface, and according to the radiation law of *Planck* the surface temperature can be deduced. In turn, the gas temperature at the HPT stator outlet  $T_{41}$  or  $SOT_P$  can be determined from the surface temperature considering the cooling effectiveness of the blade. Consequently, pyrometers measure temperatures contactless. Contrary to contact sensors, like thermocouples, they offer the following advantages: reaction to temperature changes nearly without delay, applicability at very high temperatures and non-reactivity, i.e. as the pyrometer and the blade surface have no contact, heat exchange is not taking place, thus the measured temperature is undistorted. More details about pyrometer measurements in gas turbines can be found in [1-3]. The pyrometer investigated in this work is firmly mounted in the turbine casing in front of the blade surface, as shown in Figure 1.

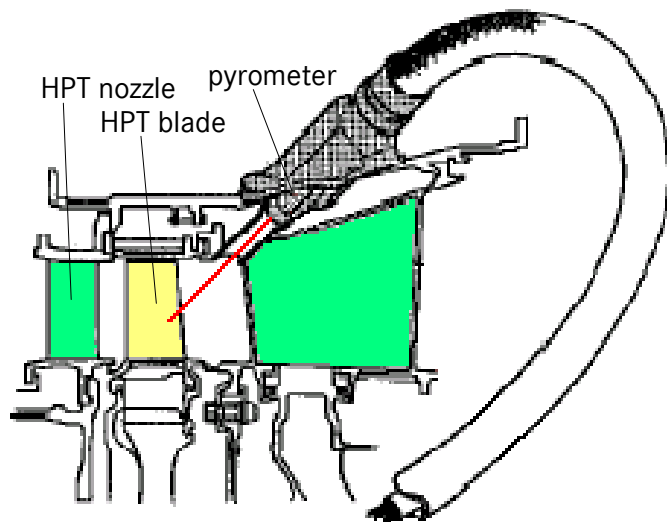


**Figure 1: HPT blade surface temperature measurement with a pyrometer**

Basically pyrometers have four parts: the optical system consisting of a lens, diaphragm and filter for capturing and imaging the radiation, the detector for transformation of the radiation into electrical signals, the evaluation unit for amplifying and linearising of the signals as well as the output unit. However, the application of pyrometers contains a number of error sources, e.g. radiations of neighbor parts, like the combustion chamber and the afterburner switch-on and -off, may be registered with the radiation of the blade. Contamination of the lens with dirt or soot particles may handicap the correct measurement of the radiation. Fitting and demounting of the pyrometer may have an adverse effect on the measurement repeatability because of the unavoidable installation tolerances. The irregular temperature profiles of the blade surface, given through the gas flow from the combustion chamber, are difficult to be sensed satisfactorily. So far these error sources cannot be eliminated, therefore an adequately large uncertainty or safety margin is necessary to avoid exceedance of the maximum allowed temperature in any case.

The two-spool engine with afterburner investigated in this work has a safety temperature margin equivalent to a wasted thrust potential of 5 %. Exhausting this potential is only possible if the temperature measurement becomes more reliable. In the following a new way for determination of the temperature  $SOT_D$  will be presented. It is based on the so-called capacity method which uses the existing standard measurements of the engine. This  $SOT_D$  is then used to online check the  $SOT_P$  from the pyrometer temperature in-flight measurement. In this work extensive engine data gained from bench and altitude test facility ATF testing as well as from flight tests has been analyzed.

## 2. The capacity method

The capacity method is a mathematical model which enables the determination of the HPT stator outlet temperature and the air mass flow of the core engine. Because of these two unknown parameters two equations are necessary. The capacity method is mainly based on two physical relationships. Firstly, on the heat balance in the control volume, which extends the high-pressure compressor exit via the combustion chamber up to the HPT stator outlet, as shown in Figure 2.

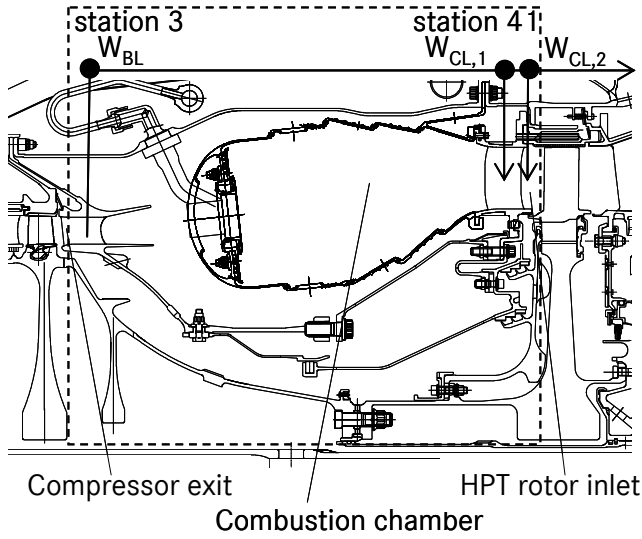


**Figure 2: Control volume for the heat balance**

The heat energy produced by the fuel flow in the combustion chamber is equal to the heat energy increase of the gas flow through the control volume. This relationship provides the following equation:

$$\Delta h_{41} - \Delta h_3 + \frac{\alpha}{\eta} \cdot (\Delta h_{41} - \Delta h_F) = \alpha \cdot h_u$$

Secondly, the fact that the HPT nozzle is choked, the flow function at the nozzle throat area, called the HPT flow capacity, is dependent on the properties of the gas only. This can be expressed as follows:

$$\frac{W_{405} \cdot \sqrt{T_{405}}}{A_{405} \cdot P_{405}} = \sqrt{\frac{\gamma}{R} \cdot \left(\frac{2}{\gamma+1}\right)^{\frac{\gamma+1}{\gamma-1}}}$$

The flow chart in Figure 3 shows the algorithm of the capacity method schematically. It considers the main influencing parameters in the control volume, i.e. secondary air flows, fuel parameters: heat value, density and temperature, effectiveness of the combustion as a function of the loading factor as well as the combustion chamber pressure loss consisting of dynamical and thermal effects. With this algorithm temperature and gas flow can be calculated iteratively, if the following input parameters are available:

- Pressure  $P_3$  and temperature  $T_3$  at compressor exit

- Fuel flow  $W_F$ , fuel temperature  $T_F$  and fuel heat value  $h_u$
- HPT nozzle throat area  $A_{405}$  and secondary air flows



**Figure 3: Flow chart of the capacity method algorithm**

As  $P_3$ ,  $T_3$  and  $W_F$  are standard measurements of every engine also in flight and the rest of the input parameters are assumed to be constant, mainly  $P_3$ ,  $T_3$  and  $W_F$  are of great importance for analyzing the accuracy of the capacity method. The calculation of  $SOT_D$  occurs in the control and monitoring unit DECU using the measurements  $W_{F,D}$ ,  $P_{3,D}$  and  $T_{3,D}$  as input. On the test-bed the measurements  $W_{F,T}$ ,  $P_{3,T}$  and  $T_{3,T}$  are also available and can be cross-checked against the DECU values to qualify first the reliability of  $SOT_D$ . The region of higher temperatures is of interest, as it contains the

thermal stress limit, which is not allowed to be exceeded. This interesting region, in which reliability of  $SOT_D$  is necessary, is defined as  $\Delta SOT_{T,ref} = SOT_T - SOT_{ref} \in [0, 200 \text{ K}]$ .

### 3. Measurement analysis and trimming

#### 3.1 Measurements and test data

In this work the data of several development engines of different standards is used, it includes:

- Several operating lines from the bench test-bed
- Several operating lines from ATF test-bed under different flight and ambient conditions
- Data from different flight missions

The measurement approaches for determination of the measured parameters available in the DECU and the comparable measured parameters available only on the test-bed are presented in the following. The DECU signal of the fuel flow is determined from the indication of the fuel metering unit of the core engine. On the test-bed the volume flow is measured with two volumetric meters, from which the fuel flow is calculated considering the effects of the fuel temperature and density. This flow value is so accurate that it can be used to calibrate the DECU signal.

The temperature at the compressor exit is measured with four rakes equipped with four thermocouples at appropriate different radial positions. The rakes are distributed in the circumferential direction and arranged at an angle of  $90^\circ$  to each other. Therefore, the temperature distribution is well recorded both in circumferential and radial directions. On the other hand, the DECU signal is not accurate enough, as it represents the value of one thermocouple only.

The registration of the total pressure is similar. On the test-bed, measurement of the total pressure at the compressor exit is performed using four rakes, each of them fitted with four probes. This guarantees a representative measurement, while the DECU signal represents a value which is deduced from the static pressure at the compressor exit measured with a single probe.

#### 3.2 Principle of test data trimming

The DECU values for  $W_{F,D}$ ,  $P_{3,D}$  and  $T_{3,D}$  are compared with and, if necessary, trimmed to those of the test-bed  $W_{F,T}$ ,  $P_{3,T}$  and  $T_{3,T}$ . For this purpose, these two kinds of values are plotted against each other and the deviations are ascertained. Only deviations of operating points are considered which are in the  $SOT$  region of interest. The deviations between the DECU values  $Y_D$  and the test-bed values  $Y_T$  were plotted against the test-bed values  $Y_T$ . For plotting referenced values were used instead of absolute ones because of the restricted data on hand. For reasons of simplicity the deviations are approximated to a line. The parameters of the lines with the gain  $a$  and offset  $b$  represent the trim parameters. The corresponding equation for the conversion of the DECU values into trimmed values is:

$$Y_T = \left\{ 1 + \frac{1}{100} \left[ \left( \frac{Y_T}{Y_{ref}} \right) a + b \right] Y_D \right\}$$

The trim parameters are calculated from the first operating line of the engine and continually applied to the following operating lines, so that the trimmed DECU values represent the input of the capacity method.

#### 3.3 Trimming of $W_{f,D}$ , $P_{3,D}$ and $T_{3,D}$

Figure 4 shows the operating lines of the same engine at standard atmosphere and sea level static conditions ISA-SLS, and Figure 5 at flight conditions. For every operating point the relative deviation between the test-bed and DECU fuel flow is plotted against the referenced test-bed fuel flow. The figures also show the trim line, which is deduced from the first operating line. Now the trimming of the fuel flow values is carried out along this line. All operating points are corrected at their corresponding abscissa location according to the trim line.

At ISA-SLS the relative fuel flow values  $W_{F,T}/W_{F,ref}$  in the  $SOT$  region of interest, are greater than or equal to 0.4, whereas at flight conditions lower values up to 0.1 are possible. As the characteristic of the fuel flows at flight conditions does not follow a straight line, the accuracy of the trimmed values will be not high enough. In this case it is convenient to define a minimum limit, e.g.  $W_{F,T}/W_{F,ref} \geq 0.375$ , in order to achieve higher accuracy. Thus the fuel flow values can be ap-

proximated to a straight line in such a way that the average accuracy of the trimmed fuel flow may increase from originally of  $2\sigma_{W_T}=\pm 5$  to  $\pm 1.5$  %.

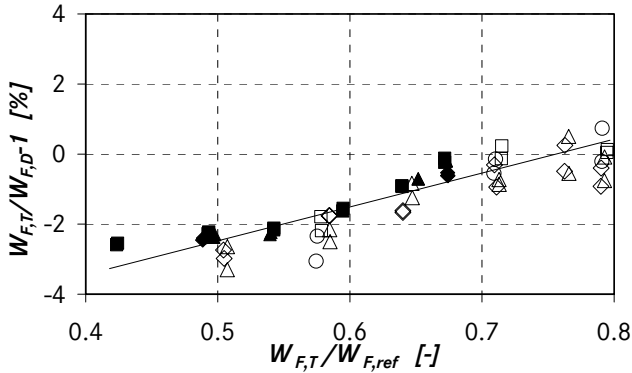


Figure 4: Fuel flow data at ISA-SLS condition with the trim line

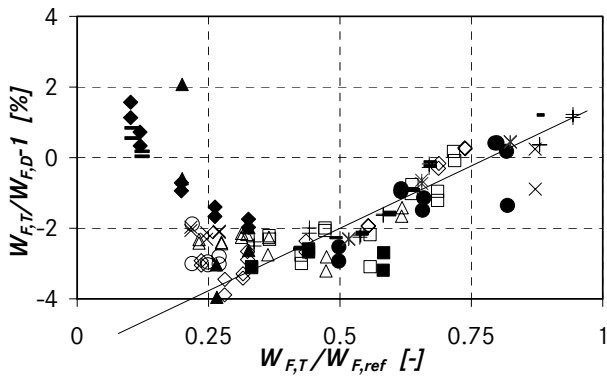


Figure 5: Fuel flow data at different flight and ambient conditions with the trim line

The trimming of the pressure at the compressor exit is performed analogously to the trimming of the fuel flow. The measured pressure values at ISA-SLS in the *SOT* region of interest are plotted in Figure 6 and those gained at different flight conditions are presented in Figure 7. Analogously to the fuel flow measurements the values at flight conditions cannot easily be approximated to a line. Therefore, the analyzed data has to be reduced. With a limitation of the pressure to  $P_{3,T}/P_{3,ref} \geq 3.4$ , for example, the data is approximately parallel to the abscissa. This results in only one value that has to be considered for trimming, i.e. the offset  $b$ . Through trimming, the pressure average error can be reduced to  $2\sigma_{P_3}=\pm 1.0$  %.

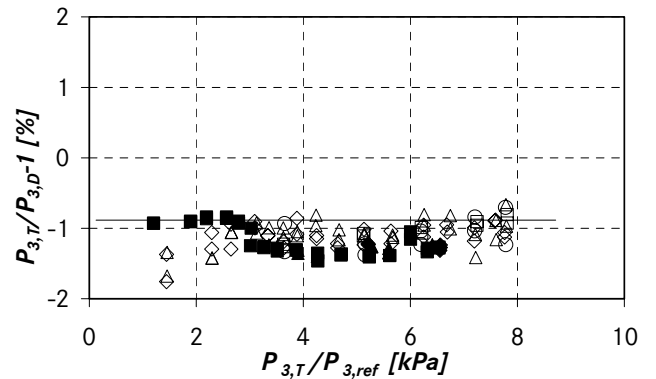


Figure 6: Compressor exit pressure at ISA-SLS condition with the trim line

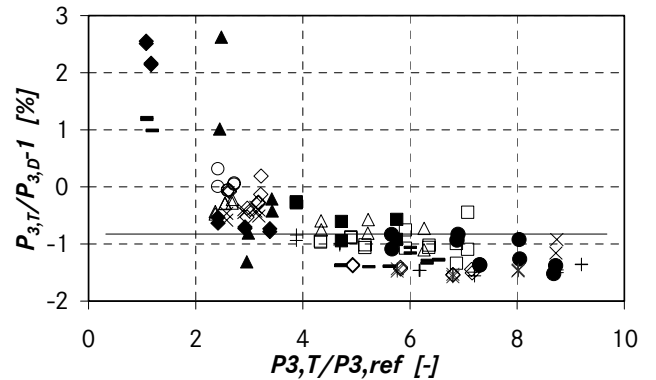


Figure 7: Compressor exit pressure at different ambient and flight conditions with the trim line

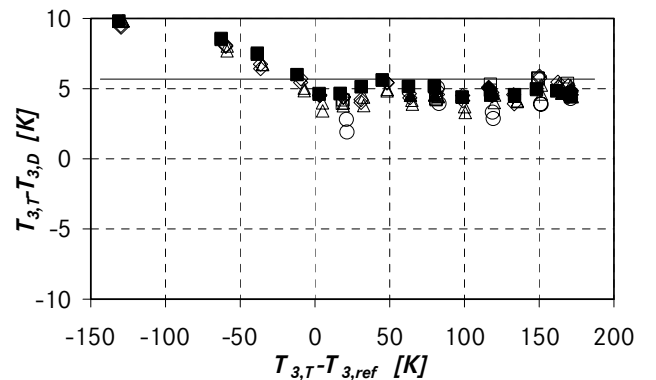
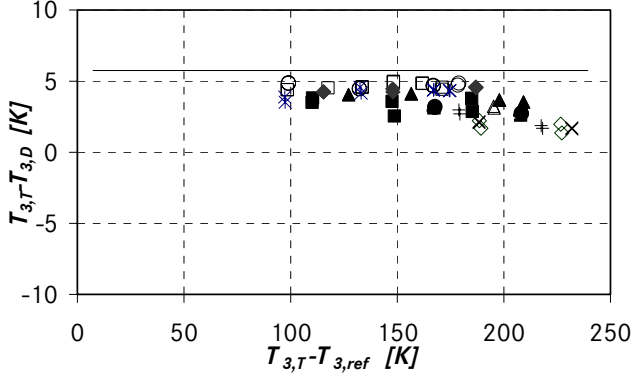


Figure 8: Compressor exit temperature at ISA-SLS condition with a trim line

The measured values of the temperature at the compressor exit are treated similarly as above. The resulting  $T_3$  data after consideration of the interesting

regions for  $\Delta SOT_{T,ref} \in [0, 200 \text{ K}]$ ,  $W_{F,T}/W_{F,ref} \geq 0.375$  and  $P_{3,T}/P_{3,ref} \geq 3.4$  is shown in Figure 8 for ISA-SLS and in Figure 9 for flight conditions. The abscissa represents the difference between  $T_{3,T}$  and a reference value  $T_{3,ref}$ , whilst the ordinate is for the difference between  $T_{3,T}$  and  $T_{3,D}$ . Due to the fact that the data is nearly parallel to the abscissa, also here only one trim parameter is sufficient to achieve an average error of  $2\sigma_{T_3} \pm 7.5 \text{ K}$ .



**Figure 9: Compressor exit temperature at different ambient and flight conditions with the trim line**

## 4. Results and discussions

### 4.1 Steady-state engine operation

Through trimming of the DECU signals it is possible to improve the accuracy of the  $SOT_D$ , which can then be used as redundancy to the  $SOT_P$  gained from the pyrometer. In chapter 3 test data from bench and ATF engine runs, representing steady-state engine operations, has been analyzed. This data shows that the following reduced errors in the DECU signals are achievable:  $2\sigma_{W_{FD}} = \pm 1.5 \%$ ,  $2\sigma_{P_{3D}} = \pm 1.0 \%$  and  $2\sigma_{T_{3D}} = \pm 7.5 \text{ K}$ , the resulting total error in  $SOT_D$  is then  $2\sigma_{SOT} = \pm 22.0 \text{ K}$ .

### 4.2 Impact of engine deterioration and configuration

The trimming of the input parameters of the capacity method is performed on the basis of the first operating line on the test-bed determining new trim parameters, which are then continually used to trim all operating points till the engine is again on the test-bed. Continued accuracy of the calculated  $SOT_D$  is of great importance in the time between two overhauls, where the

engine may deteriorate. To analyze this, an engine endurance test may be suitable. The data of an endurance test of 150 hours has been analyzed to determine, whether the accuracy over the whole running time remains unchanged or not. Totally, after certain intervals, ten operating lines have been tested. From the first operating line the trim parameters have been determined, which are then used to trim the input parameters  $W_{F,D}$ ,  $P_{3,D}$  and  $T_{3,D}$  of the capacity method for all ten operating lines.

In Figure 10 the deviations between the  $SOT_D$  from the trimmed DECU values and the  $SOT_T$  calculated from the test-bed values for all operating points of each operating line are plotted. The deviations amount to between  $2\sigma_{SOT} = \pm 2.5$  and  $\pm 12 \text{ K}$  and do not show a clear trend, indicating that there is a running time dependent inaccuracy.

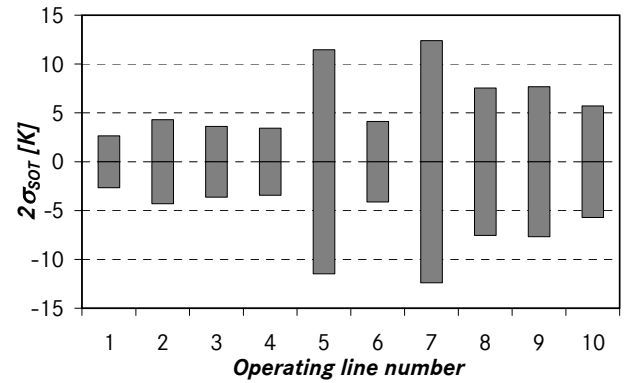


**Figure 10: Development of the SOT accuracy during an endurance test**

Also of interest is, whether the repeatability of the  $SOT_D$  accuracy is given for all engines when using the trim parameters. For this purpose, the test data of five engines have been investigated. For each set of test data the trim parameters have been determined and then used to trim the input parameters  $W_{F,D}$ ,  $P_{3,D}$  and  $T_{3,D}$ . In turn the average errors  $2\sigma_{W_{FD}}$ ,  $2\sigma_{P_{3D}}$  and  $2\sigma_{T_{3D}}$ , and from these  $2\sigma_{SOT}$  are calculated for each engine using trade factors obtained from the capacity method algorithm. The results are shown in Table 1, where the error  $2\sigma_{SOT}$  has values between  $\pm 16.35$  and  $\pm 20.85 \text{ K}$ . These deviations are also so small that the same trim parameters can be used for all engines.

Engine	$\pm 2\sigma_{WFD}$	$\pm 2\sigma_{P3D}$	$\pm 2\sigma_{T3D}$	$\pm 2\sigma_{SOT}$
1	1.32	0.41	9.05	17.70
2	1.14	0.69	7.31	16.35
3	1.52	1.05	5.47	20.85
4	1.31	0.76	3.96	17.03
5	1.43	1.09	6.31	20.59

**Table 1: The accuracies of the trimmed parameters and the resulting SOT accuracy of different engines**

#### 4.3 Impact of engine transient

In order to compare the temperature  $SOT_D$  of the capacity method with the temperature  $SOT_P$  from the pyrometer, flight data have been investigated. Figure 11 shows a typical flight trajectory, the interesting temperature region is marked on the plot. It contains the climb, flight at higher altitude and at higher Mach numbers. To investigate this region deeper, the corrected relative rotational speed of the low-pressure compressor  $N_{L,C}$  is plotted against the flight time  $t$  in Figure 12, showing that apart from regions with somewhat stable speeds regions with sudden speed changes exist as well.

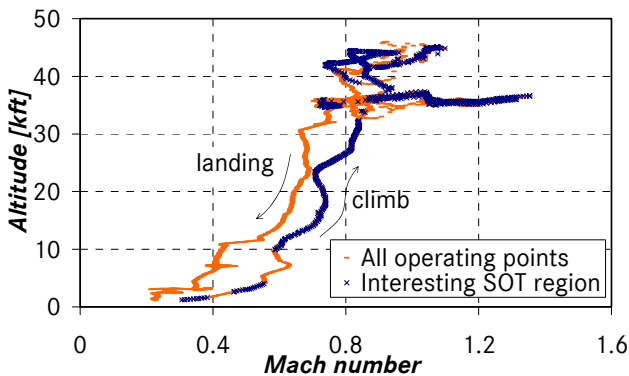


**Figure 11: A typical flight trajectory**

As shown in Figure 13 for the same flight trajectory segment, the temperature difference  $\Delta SOT_{D,P} = SOT_D - SOT_P$  is also plotted versus the flight time. It is noticeable that in regions with more marked speed changes there are also major  $\Delta SOT_{D,P}$  variations. In transient cases where the speed changes occur suddenly, the deviation between  $SOT_D$  and  $SOT_P$  is so big that the check of  $SOT_P$  via  $SOT_D$  is only partially possible, namely through introduction of time intervals in which

the speed change does not exceed a certain value. If only the data is considered, which fulfills the criterion  $\Delta N_{L,C}/\Delta t \leq 0.5 \text{ %/s}$ , then the plots in Figure 14 will result. In this case, the deviations between the temperatures can be decreased to about  $\pm 25 \text{ K}$ . With the application of such a criterion the  $SOT_P$  check via  $SOT_D$  remains possible also for transient flight cases, however some segments of the flight trajectory may be excluded.

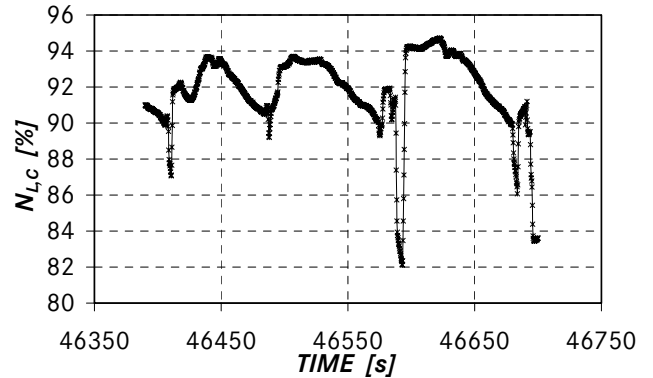


**Figure 12: Low-pressure spool speed versus flight time for a flight trajectory segment**

Data of another flight mission is presented in Figure 15. It shows that there are big temperature deviations of up to 100 K, especially at the beginning of an engine load change despite the use of the criterion  $\Delta N_{L,C}/\Delta t \leq 0.5 \text{ %/s}$ . This can be lead back to the fact that the blade surface temperature measured by the pyrometer is very inert. Improvement can only be achieved through a transient model, which describes the blade surface temperature behavior.

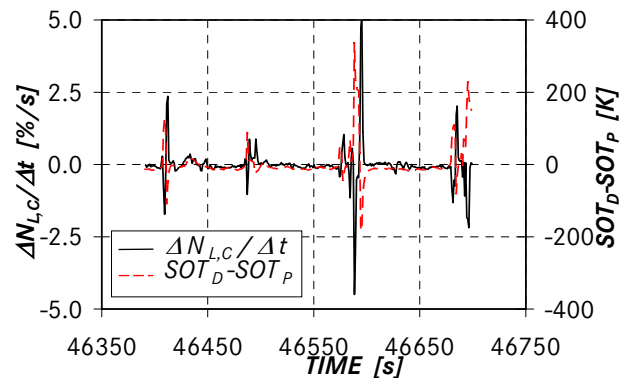


**Figure 13:  $\Delta N_{L,C}/\Delta t$  and  $SOT_D - SOT_P$  change**

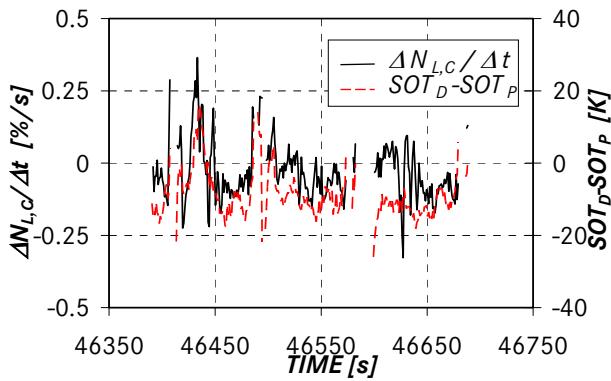


**Figure 14: Change of  $SOT_D$  against  $SOT_P$  after use of the  $\Delta N_{L,C}/\Delta t \leq 0.5$  %/s**

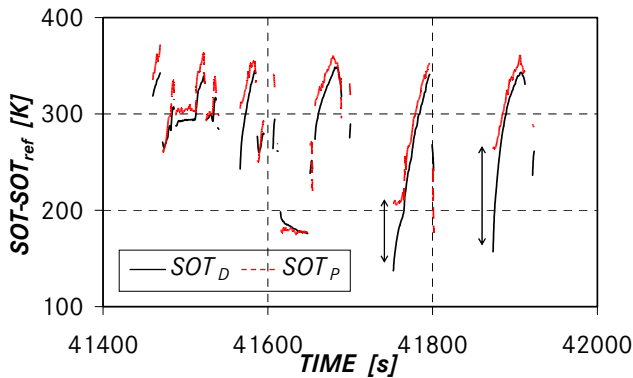


**Figure 15: At the beginning of a load change the difference between  $SOT_D$  and  $SOT_P$  is large**

## 5. Concluding remarks

The temperature at the inlet of the high-pressure turbine is very important for monitoring and control purposes, because modern engines are subjected to stresses nearly as high as the stress limits of the materials. To determine this temperature pyrometers are used, however there exist repeatability and accuracy problems. To overcome these problems the engine standard analyzed in this work needs an uncertainty margin of 50 K in the HPT stator outlet temperature  $SOT$ , which is equivalent to a thrust potential loss of 5 %.

In this work a new way based on the capacity method for determination of a redundant temperature has been presented, which can be used to online check the temperature deduced from the pyrometer measurements in flight. This may decrease the necessary uncer-

tainty margin to 22 K leading to a thrust potential gain of 3 %. This is especially valid for steady-state flight. Through applying stability criteria at moderate engine load changes this uncertainty margin can be maintained.

During severe transients the deviations between the temperatures calculated from the pyrometer measurements and those from the capacity method are so large that a solution appears to be difficult. This problem is mainly attributable to the fact that the blade surface temperature is inert. A temperature check in all flight cases requires a transient model which considers all relevant physical relationships. This should be the subject of future works.

## Acknowledgments

This paper is based on a thesis research work that was sponsored by MTU Aero Engines GmbH. The authors owe Jochen Kurzak a debt of gratitude for his intensive support. Further the authors would like to express their sincere gratitude to their colleagues at MTU, who were always available for discussions about this work.

## References

- [1] Suarez E., Prziembel H. R. Pyrometry for Turbine Blade Development. AIAA-88-3036, Boston, 1988
- [2] Eggert T. Turbinenpyrometrie mit hoher örtlicher und zeitlicher Auflösung. Wissenschaft & Technik Verlag, Berlin, 1999
- [3] Kerr C., Ivey P., Oxley N. Computational Comparison of the RB199 and GE90 Pyrometer Purging Systems. ASME GT-2002-30049, 2002